Analysis of small droplets with a new detector for liquid chromatography based on laser-induced breakdown spectroscopy. Spectrochim. Acta B 60, 993–1001

ARTICLE *in* SPECTROCHIMICA ACTA PART B ATOMIC SPECTROSCOPY · AUGUST 2005

Impact Factor: 3.18 · DOI: 10.1016/j.sab.2005.05.033

ELSEVIER

Spectrochimica Acta Part B 60 (2005) 993 – 1001

SPECTROCHIMICA ACTA PART B

www.elsevier.com/locate/sab

Analysis of small droplets with a new detector for liquid chromatography based on laser-induced breakdown spectroscopy☆

Christoph Janzen [a,*], Rüdiger Fleige [a], Reinhard Noll [a], Heinrich Schwenke [b], Wilhelm Lahmann [b], Joachim Knoth [b], Peter Beaven [b], Eckard Jantzen [c], Andreas Oest [c], Peter Koke [d]

[a] *Fraunhofer-Institut für Lasertechnik (ILT), Steinbachstr. 15, D-52074 Aachen, Germany*
[b] *GKSS-Forschungszentrum Geesthacht GmbH, Max-Planck Str. 1, D-21502 Geesthacht, Germany*
[c] *GALAB, Max-Planck-Strasse 1, D-21502 Geesthacht, Germany*
[d] *OBLF Gesellschaft für Elektronik und Feinwerktechnik mbH, Salinger Feld 44, D-58454 Witten, Germany*

Received 30 November 2004; accepted 30 May 2005
Available online 23 June 2005

Abstract

The miniaturization of analytical techniques is a general trend in speciation analytics. We have developed a new analytical technique combining high pressure liquid chromatography (HPLC) with laser-induced breakdown spectroscopy (LIBS). This enables a molecule-specific separation followed by an element-specific analysis of smallest amounts of complex samples. The liquid flow coming from a HPLC pump is transformed into a continuous stream of small droplets (diameter 50–100 μm, volume 65–500 pl) using a piezoelectric pulsed nozzle. After the detection of single droplets with a droplet detector, a Q-switched Nd:YAG Laser is triggered to emit a synchronized laser pulse that irradiates a single droplet. The droplets are evaporated and transformed to the plasma state. The spectrum emitted from the plasma is collected by a spherical mirror and directed through the entrance slit of a Paschen–Runge spectrometer equipped with channel photomultipliers. The spectrometer detects 31 elements simultaneously covering a spectral range from 120 to 589 nm. Purging the measurement chamber with argon enables the detection of vacuum–UV lines. Since the sample is transferred to the plasma state without dilution, very low flow rates in the sub-μl/min range can be realised.

Keywords: LIBS; HPLC; Droplet analysis

1. Introduction

1.1. Motivation for a new hyphenated technique: HPLC–LIBS

The LIBS technique allows the chemical analysis of substances in all different states of aggregation. Under special conditions, the elemental compounds in liquids can also be analyzed with high sensitivity[1]. This suggests the use of LIBS for a field of growing interest in the analytical sciences, speciation analysis [2,3].

The chemical, biological and toxicological properties of many elements are critically dependent upon their chemical form, its oxidation number and the compound the element is occurring in. This has a great impact on environmental and biological chemistry, occupational health, nutrition and medicine. Typical targets of speciation analysis are metal ions in different oxidation states, metal complexes with inorganic and organic ligands, metalloid oxoanions, organo-metallic compounds and ionic nonmetal species. An analytical technique yielding only the total amount of the

☆ This paper was presented at the 3rd International Conference on Laser Induced Plasma Spectroscopy and Applications (LIBS 2004), held in Torremolinos (Málaga, Spain), 28 September – 1 October 2004, and is published in the special issue of *Spectrochimica Acta Part B*, dedicated to that conference.

* Corresponding author. Tel.: +49 241 8906 0.
E-mail address: christoph.janzen@ilt.fraunhofer.de (C. Janzen).

0584-8547/$ - see front matter © 2005 Elsevier B.V. All rights reserved.
doi:10.1016/j.sab.2005.05.033

analyzed element does not consider different possible forms. Coupled techniques combining chromatographic separation with element-specific detection have therefore become fundamental tools for speciation analysis. These so-called "hyphenated techniques" enable the elemental analysis of separated fractions of complex samples. Typical detection techniques are mass spectrometry or atomic absorption and atomic emission spectrometry and the most common separation techniques are gas chromatography (GC) for volatile compounds and high pressure liquid chromatography (HPLC) for less volatile compounds. In recent years capillary electrophoresis has also become more and more important in this field [4].

Table 1 gives an overview of the most important hyphenated techniques and their status of applicability.

The detection procedure should give maximum information with minimum sample consumption. The LIBS process as a detection technique offers several significant advantages: LIBS signals yield the elemental composition of complex samples, the plasma breaks up any molecular structure and the individual elements lead to specific radiation. The information content is therefore higher than with the UV-VIS or fluorescence detectors that are frequently used in HPLC chromatography. LIBS is a true multi-element technique. Depending on the spectrometer used, several elements can be monitored at the same time without loss of sensitivity. Today ICP-MS detectors (inductively-coupled plasma mass spectrometry) are used to achieve highest sensitivity, making sample concentrations as low as pg/g (ppt) possible [5,6]. Plasma generation is achieved with the aid of an inductively heated argon torch, the sample is diluted in a large amount of gas needed for the plasma generation (typically several liters per minute). ICP-MS detectors achieve their highest sensitivity working with flow rates in the range of ml/minute, which fit well to HPLC. Significantly lower flow rates lead to a loss in sensitivity.

With LIBS the sample is transferred directly into the plasma state, without the need for an additional gas flow. No dilution of the sample occurs and the method is capable to analyze sample amounts as low as a few nanoliters. This will turn out to be valuable for the coupling with low flow separation techniques such as capillary electrophoresis or micro-HPLC. In these separation techniques only a few µl/minute are needed.

Table 1
Different hyphenated techniques

	GC	HPLC	SFC	HPTLC	CE
MS	♦♦♦	♦♦♦	♦	♦	♦♦
IR	♦♦♦	♦♦	♦	♦♦	♦
OE	♦♦	♦	♦		
AAS	♦	♦♦			
NMR		♦♦			♦
Fluorescence	♦♦	♦♦♦		♦♦♦	♦♦♦
UV-VIS	♦	♦♦♦		♦♦♦	♦♦♦

Separation: GC (gas chromatography), HPLC (high pressure liquid chromatography), SFC (supercritical fluid chromatography), HPTLC (high performance thin layer chromatography), CE (capillary electrophoresis). Detection: MS (mass spectrometry), IR (infrared spectrometry), OE (optical emission), AAS (atomic absorption spectrometry), NMR (nuclear magnetic resonance), fluorescence spectrometry, UV-VIS spectrometry.
♦♦♦ Standard technique.
♦♦ Commercially available, less spread.
♦ Experimental status, not commercially available.

1.2. LIBS analysis in aqueous media

Water is one of the common solvents in HPLC chromatography and therefore the process of plasma generation using aqueous samples must be well understood. The mechanisms of plasma formation in water have been thoroughly examined and different theoretical models to describe the breakdown have been published (multiphoton model, cascade model) [7].

Different setups to record laser-induced breakdown spectra in a water matrix have been described in the literature: bulk analysis in cuvettes [8] or on the liquid surface [9], the analysis of liquid jets [10], aerosols [11] or the analysis of single, isolated droplets [12]. Plasma formation in bulk water generally suffers from short lifetimes such that the emission intensity falls steeply after approximately 1µs, making sensitive measurements impossible [13]. Pichahchy et al. [14] compared single and double pulse LIBS spectra from metal samples placed under water and showed that only the double pulse arrangement provides sufficient excitation to identify the sample compounds. With a single pulse, the plasma formed is surrounded by an aqueous medium that leads to a fast decay of the plasma radiation. In the double pulse experiment, the first pulse produces a gaseous atmosphere in which the second pulse, reaching the target some 10 µs later, produces a plasma with a significantly longer lifetime. The excitation of the plasma in air or noble gas atmospheres yields larger signal intensities than plasma generation inside bulk water, this can also be seen in single pulse experiments [15]. Thin water jets, aerosols or single, isolated droplets are superior sample forms compared to bulk water, because the plasma can expand in a gaseous atmosphere.

Using a water film and a dual-beam dual-pulse setup Kuwako et al. could demonstrate a limit of detection as low as 0.1 ppb for sodium in water [16]. An alternative approach to obtain a very high sensitivity was made by Lo and Cheung, who used an ArF-Laser at 193 nm for excitation instead of the commonly used YAG Laser (1064 nm). Limits of detection in the low ppb region were achieved for sodium, calcium and barium as a result of the efficient photo-ionization of hot water molecules by the UV photons [17].

1.3. The concept of HPLC–LIBS

Fig. 1 shows a diagram of the new analytical hyphenated technique HPLC–LIBS. The HPLC output is fed into the droplet generator and transformed into a continuous stream of uniform droplets.

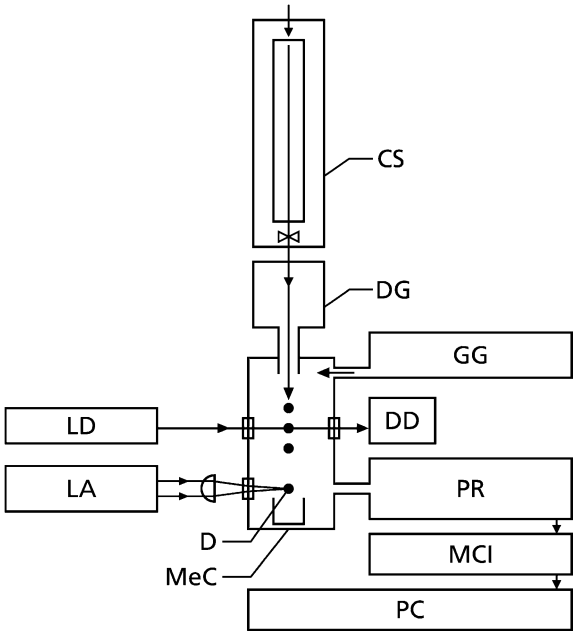

Fig. 1. Setup for HPLC–LIBS. The eluate of the chromatographic separation (CS) is fed into a droplet generator (DG) that produces a continuous stream of droplets (D). Individual droplets are detected by a unit consisting of a laser diode (LD), an achromatic lens and a photodiode for droplet detection (DD). The detection of a droplet triggers a Q-switched Nd-YAG laser (LA), the laser pulse transforms a single droplet into the plasma state, the radiation is guided into a Paschen–Runge spectrometer (PR) and analyzed by a multi-channel integrator electronics (MCI). Measurements are stored and processed in a computer (PC). A gas guiding system (GG) leads argon into the measurement chamber (MeC).

In order to achieve the best possible transfer of sample material into the plasma we chose to apply a single droplet generator based on a piezoelectric nozzle. Unlike electrospray or aerosol generators a piezoelectric nozzle is a "drop on demand" device that produces single, isolated droplets with volumes typically between 100 pl and 1 nl and an initial velocity of 1–2 m/s. By synchronizing laser pulses to single droplets we generate plasmas in a gaseous environment. The process of droplet formation is highly reproducible, leading to a uniform droplet size. Phase Doppler anemometry measurements performed with a piezoelectric droplet generator similar to the one used in this work revealed a relative standard deviation of the droplet volume of 3% for droplets of 86 μm diameter [18]. After detection of an individual droplet the laser is triggered and emits a single Q-switched pulse that is focused onto the droplet and generates a plasma. The plasma radiation is collected and guided to the spectrometer.

2. Experimental setup

Fig. 2 shows the optical setup for the analysis of single picoliter droplets. For a better control of the experimental parameters the HPLC was replaced by a stock of sample solution, having a constant analyte concentration. Prior to analysis all samples were filtered through 0.2 μm pore size membrane filters. The plasma radiation is resolved spectrally with a Paschen–Runge spectrometer (type: QSN 750

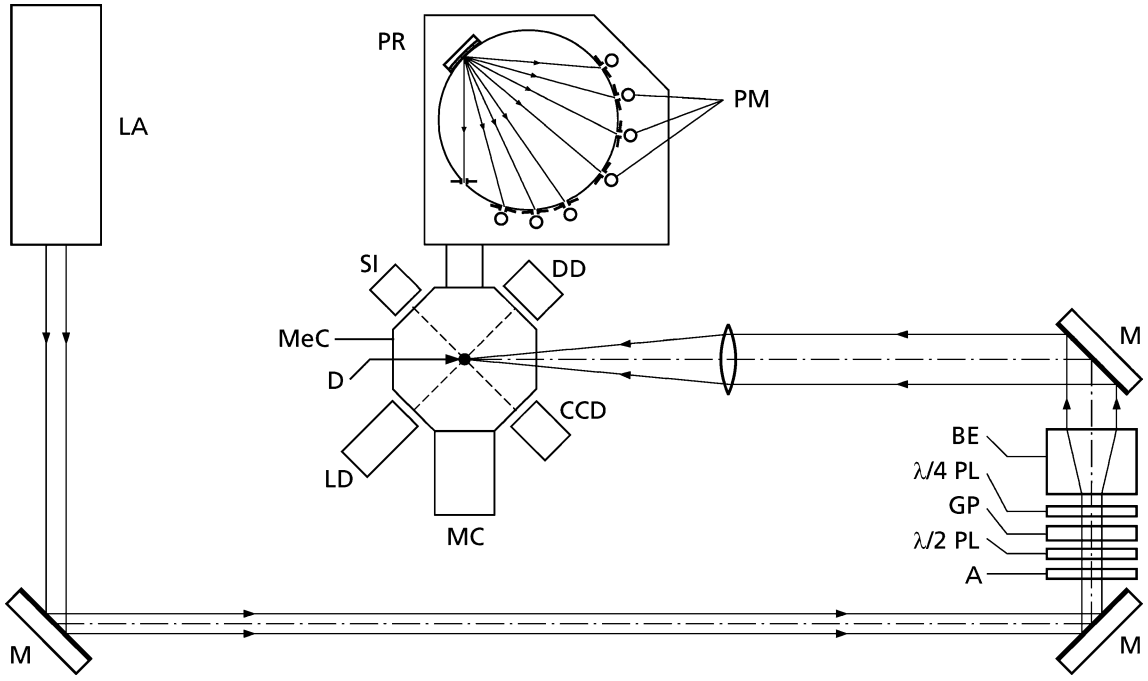

Fig. 2. Optical setup for LIBS experiments on droplets. M=mirror, LA=laser, A=aperture, λ/2 PL=λ/2 plate, λ/4 PL=λ/4 plate, GP=Glan laser-polarizer, BE=beam expander, D=droplet, MC=mirror chamber, MeC=measurement chamber, CCD=CCD-camera for droplet observation, DD=droplet detector (photodiode), SI=stroboscopic illumination, LD=laser diode (part of the droplet detector), PM=photomultiplier.

from OBLF; Witten, Germany) equipped with 33 channel photomultipliers (type C 932, C 933, C 911 from Perkin Elmer), enabling the simultaneous detection of 31 different elements and the zeroth order signal. Among these elements are non-metals such as Ar, H, C, O, N, P, S, alkali and alkaline earth metals (Na, Ca, Mg) and various metals that play a significant role in the fields of environmental chemistry, clinical biochemistry, industrial chemistry, nutrition and toxicology as e.g., As, Hg, Cr, Pb and Pt. Most of these elements can form different metalloid species. The choice of elements for the Paschen–Runge spectrometer was made to guarantee a broad spectrum of possible chromatographic applications for the new LIBS detector. The non-metal elements could be used for the analysis of organic substances. Because all elements have multiple transitions a careful choice of the lines that are best suited for the analysis is important. We analyzed most of the mentioned elements by recording laser induced breakdown spectra with an echelle spectrometer. The matrix the element is surrounded by might affect the line intensities, therefore all echelle spectra were recorded from small water droplets containing diluted samples. Usually the line showing the strongest intensity was chosen. A complete list of all elemental transitions detectable with the Paschen–Runge spectrometer is given in Table 2.

The plasma emission shows a strong continuum peak directly after the laser pulse irradiation that decays faster than the element specific line emission. After a few microseconds, only the element-specific line emissions can be detected. For a better signal-to-noise-ratio the continuum part of the plasma emission is excluded from the analytical signal with the aid of gated signal integration. Typical delay times between the laser pulse and the start of the signal integration are 0.5–1.5 μs, the integration gate width is between 20 and 50 μs. The photomultiplier signals are processed by a multi-channel integration electronics (MCI, developed by the Fraunhofer-Institute for Laser Technology), the photocurrent from 33 photomultipliers can be integrated simultaneously with individual time gates. A description of the MCI is given in Noll et al. [19]. For single pulse evaluation the signal intensities of all channels are transmitted to a computer. The multi-channel integration electronics allows fast measurement frequencies of up to 1000 Hz with single pulse evaluation.

In order to select the elemental transitions with the best analytical performance, we studied laser-induced breakdown spectra of droplets between 200 and 780 nm with an echelle spectrometer (type ESA 3000 from Laserlabor Adlershof, Berlin, Germany) for each element. The experimental setup for the selection of the transitions was similar to the one described here except that the spectrometer was connected to the experiment with a fiber optics.

In order to achieve higher signal intensities, the plasma emission is collected with a spherical mirror and focused on the entrance slit of the Paschen–Runge spectrometer. The mirror is placed inside the measurement chamber and can be adjusted without opening the chamber. The droplet generator is also placed in the measurement chamber and produces a free falling stream of droplets. It is made of a glass capillary with a small orifice (50 μm diameter) on one side that is enclosed by a tube-shaped piezoelectric element. The piezoelectric element is activated with a voltage pulse that induces a pressure wave in the liquid leading to the formation of a single isolated droplet with a volume between 100 pl and 1 nl and an initial velocity of 1–2 m/s. A CCD camera with a stroboscopic illumination is used to control and adjust the droplet generation. Fig. 3 shows the droplet generator and uniform droplets under stroboscopic illumination. The piezoelectric nozzle is capable of delivering up to 2000 droplets per second, however, droplet frequencies as low as 10–20 Hz are also possible. The droplet size can only be varied in a narrow range by adjusting the voltage pulse. A higher peak voltage leads to a higher droplet speed, larger pulse length leads to larger droplets. Every individual piezoelectric nozzle has a set of parameters it is giving the best performance with (best stability and droplet uniformity)

Table 2
List of all element lines installed in the Paschen–Runge spectrometer

Element	Wavelength [nm]	Energy lower state [eV]	Energy upper state [eV]	Grating order
P	178.28	0.0000	6.9548	1
S	180.73	0.0000	6.8606	1
Se	196.09	0.0000	6.3232	1
Zn	213.86	0.0000	5.7961	1
Sb	217.59	0.0000	5.6969	1
Cd	228.80	0.0000	5.4175	1
As	234.98	1.3134	6.5884	1
H	121.57	0.0000	10.1995	2
B	249.77	0.0019	4.9646	1
Si	251.61	0.0277	4.9541	1
Hg	253.65	0.0000	4.8868	1
O	130.22	0.0000	9.5220	2
Pt	265.94	0.0000	4.6600	1
Mg	279.55	0.0000	4.4341	1
N	149.26	2.3837	10.6900	2
V	310.23	0.3680	4.3637	1
Sn	317.50	0.4250	4.3291	1
Cu	324.75	0.0000	3.8169	1
C	165.70	0.0054	7.4883	2
Ti	334.94	0.0488	3.7496	1
Ni	341.48	0.0254	3.6554	1
Co	345.35	0.4318	4.0212	1
Cr	357.87	0.0000	3.4638	1
Fe	371.99	0.0000	3.3322	1
Al	394.40	0.0000	3.1429	1
Ca	396.85	0.0000	3.1236	1
Ce	399.92	0.2954	3.3949	1
Pb	405.78	1.3206	4.3754	1
Ar	420.07	11.5491	14.5000	1
La	433.37	0.1729	3.0332	1
H	486.13	10.1995	12.7494	1
Na	589.00	0.0000	2.1024	1
0th order				0

The choice of the respective transitions was made on the basis of measurements with an echelle spectrometer.

and the nozzles show little tolerance for deviations from these parameters. Therefore systematic studies with droplets of different sizes were not accomplished.

A droplet detection unit consisting of a diode laser, an achromatic lens and a photodiode is used to detect single droplets with a temporal precision of approximately 1 μs. The photodiode signal shows a characteristic "W" shape, when the droplet trajectory passes through the focus of the diode laser beam. This can be exploited for precise adjustment of the droplet in space and time. The photodiode signal is shown in Fig. 4. The shape of the signal can be explained with the droplet being a small sphere that does not refract light when the beam focus lies in the center of the sphere, so the loss of photodiode signal due to the droplet is minimized in this moment.

After detection of a droplet, a synchronized laser pulse is emitted that transforms the droplet into a plasma. Temporal and spatial overlap between laser pulse and droplet are essential for a stable analytical signal. Temporal misalignment of a few microseconds or spatial misalignment of a few micrometers leads to a significant decrease in signal intensity. We used a Q-switched Nd-YAG laser (Continuum Surelight, 10 ns pulse width, 10 Hz repetition rate) for the experiments described in this paper. The repetition rate of the laser restricts the measurement frequency to 10 Hz, although the other components of the experiment (droplet generator, spectrometer, signal integration and recording) could permit measurements at a rate of 1000 Hz. The laser pulses were attenuated with the aid of a Glan laser-polarizer and a $\lambda/2$-plate to 50–140 mJ. The laser beam is expanded to a diameter of approximately 3 cm and then focused with an achromatic lens having a focal length of 10 cm. For adjustment, the lens can be translated perpendicularly to the laser beam and in the direction of the laser beam. For the timing of the signal detection and the laser trigger relative to the droplet detection a digital delay generator (Stanford DG 535) was used.

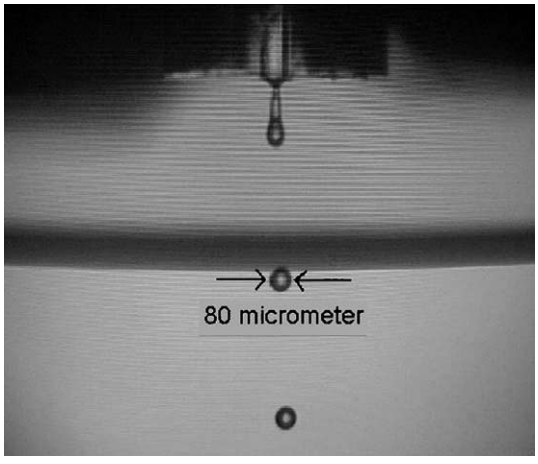

Fig. 3. Image of 270 pl droplets. The picture was taken with stroboscopic illumination, the droplet formation frequency is approximately 800 Hz. A part of the glass capillary of the droplet generator can be seen in the upper part of the picture.

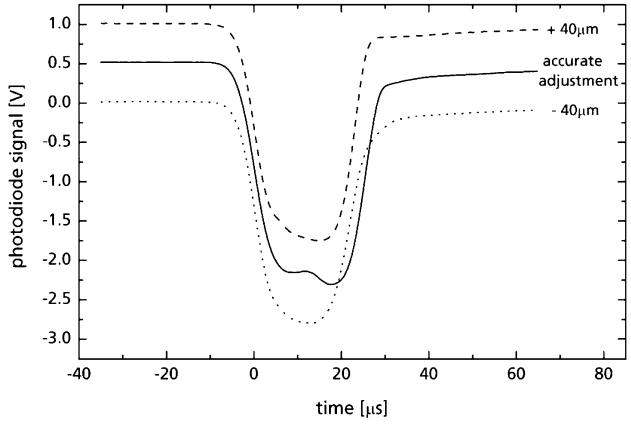

Fig. 4. Photodiode signal for different positions of the droplet. When the droplet passes through the focus of the diode laser beam the characteristic "W" shape can be seen. A lateral displacement of 40 μm leads to the two additional signals shown. In case of the accurate adjustment the rise in signal intensity in the center of the peak can be explained with the droplet being a small sphere that does not refract light when the beam focus lies in the center of the sphere and all rays are propagating perpendicularly through the surface of the sphere.

3. Measurements

3.1. Analysis of plasma dynamics

For a better understanding of the interaction between laser pulse and droplet the plasma dynamics was studied with an electro-optical high speed camera enabling exposure times down to 200 ps (Stanford Computer Optics, 4 Picos). A 500 ppm sodium solution was used to produce intense element-specific radiation. An interference filter (central wavelength 589 nm, FWHM 10 nm) placed in front of the camera transmits the radiation coming from the sodium transitions at 589.00 and 589.59 nm. A series of images recorded with a shutter time of 80 ns with varying delay times is shown in Fig. 5, the hair cross indicates the initial position of the droplet. The laser beam (50 mJ pulses, 10 ns pulse width) enters from the right side and the focus position is a few millimeters behind the droplet. Every picture has a size of 5 mm * 3.75 mm.

The first breakdown can be detected at the rear side of the droplet because the beam is focused by the droplet itself leading to the highest laser intensity at the rear side of the droplet. During the first 500 ns of expansion (not shown here) the breakdown moves in the direction of the laser beam, because evaporated material is further heated by the laser pulse. The intensity distribution of the plasma radiation is asymmetric with the side facing the laser emitting most of the radiation. The plasma grows within 500 ns to a diameter of approximately 2.5 mm. No fragmentation of the droplets was observed on the images. We measured the diameter of

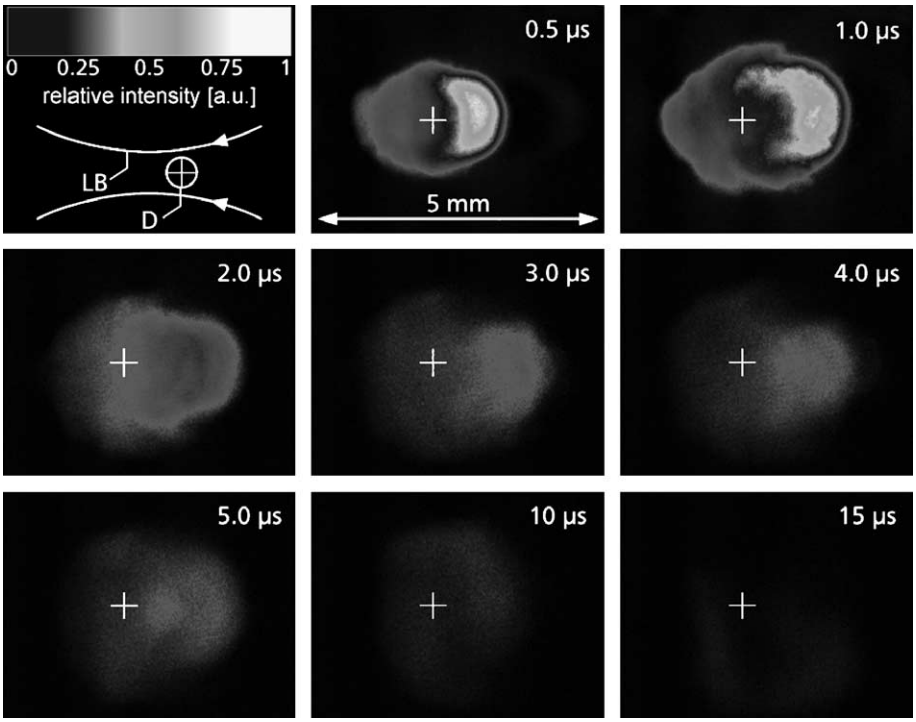

Fig. 5. Development of the plasma recorded with an electro-optic camera. Sample: 500 ppm sodium solution. Shutter time: 80 ns. Interference filter: center at 589 nm, FWHM 10 nm. Laser pulse: 50 mJ, 10 ns, focus 5 mm behind droplet. The upper left picture shows the relative positions of laser focus and droplet, the initial droplet position is marked with a reticle in all pictures. Delay times relative to the start of the laser pulse are given for each picture. LB = laser beam, D = droplet.

the luminous plasma as a function of time and calculated the speed of propagation which decreases from 40 km/s during the first nanoseconds of the expansion to less than 1 km/s after 500 ns, see Fig. 6. Two regions with a different dynamic behavior can be distinguished. Between 15 and 30 ns the expansion can be fitted by a linear regression described by the function $d \sim t^{1.860.3}$ (d = plasma diameter), between 100 and 500 ns the linear fit yields $d \sim t^{1.860.3}$. It must be pointed out that we did not analyze the expansion of the shock wave which can be described by the Sedov model

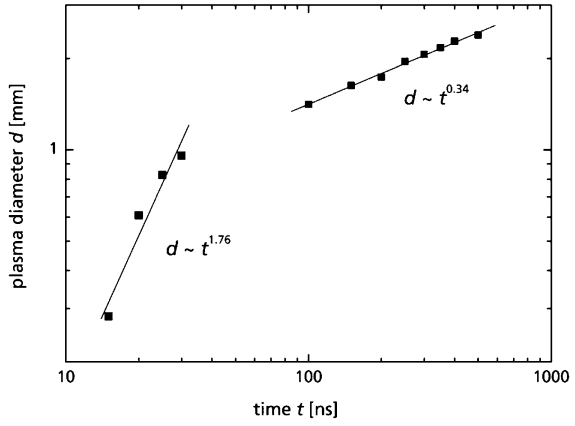

Fig. 6. Plot of the plasma expansion for the first 500 ns. The speed of the expansion drops from 40 km/s during the first nanoseconds to less than 1 km/s after 500 ns. Two different expansion regimes can be distinguished that follow two different power laws.

[20], but the expansion of the luminous plasma front. Normally the plasma front is retarded relative to the shock wave. An example for the analysis of shock waves produced during a LIBS experiment is given in Noll et al. [21].

In consideration of the heat capacity of liquid water (4,18 J/g*K) and the enthalpy of vaporization (2258 J/g at 100 °C) it takes approximately 0.7 mJ to vaporize 270 pl of liquid water. With the laser pulse having an energy of 50 mJ sufficient energy is available for complete vaporization. From the fast expansion and the homogeneity of the plasma we see no hints for any fragmentation into smaller sub-droplets or parts of the droplet which are not transferred to the plasma state.

3.2. Optimization of the measurement parameters

In a series of experiments we analyzed the influence of the laser pulse energy and wavelength on the analytical sensitivity. We used the fourth harmonic of a Nd-YAG Laser (266 nm) to perform LIBS experiments with small droplets and compared the results to the excitation with 1064 nm. For both wavelengths calibration curves with different sodium concentrations between 0 and 10 ppm were measured and the limits of detection were compared. With 60 mJ pulses at 1064 nm a limit of detection of 0.75 ppm was calculated using the 3s-criterion [22]. The same measurements were made with 25 mJ pulses at 266 nm and yielded a limit of detection of 2 ppm. When using the same pulse energy (25

mJ) for both wavelengths, the signal intensities of the sodium 589.00 and 589.59 nm lines are approximately twice as high with the excitation at 266 nm compared to the 1064 nm excitation. Since the laser could not deliver more than 25 mJ of the UV wavelength per pulse, we used the fundamental wavelength in all subsequent experiments.

The signal intensities show a strong correlation to the laser pulse energy. Fig. 7 shows the rise of the line intensities of sodium lines for 500 ppm sodium droplets with the laser pulse energy. For more than 60 mJ/pulse a saturation of the line emission is observed. Since very high pulse energies can lead to instabilities in the operation of the piezoelectric droplet generator, most measurements were performed in the range between 60 and 100 mJ/pulse.

3.3. Analytical sensitivity

In order to determine the analytical sensitivity we recorded echelle-spectra from different samples containing between 0 and 0.7 μg/g calcium. Samples were diluted from a 100 ppm stock solution containing Ca stabilized with 5% nitric acid. The average integral intensity of 20 measurements, with each measurement consisting of 100 droplets, is plotted as a function of the concentration in Fig. 8. Integral intensities were calculated by fitting a Gaussian function to the calcium peak at 393.37 nm and subtracting the background intensity (baseline subtraction). The concentration with the same signal intensity as three times the standard deviation of the zero-sample, the limit of detection [22], is calculated to be 20 ng/g.

This detection limit is higher than those obtained with ICP-MS systems. Many elements can be detected in the range of low ppt values with modern ICP-MS systems [5,6]. Nevertheless, the absolute sensitivity of our experimental setup is very high, for elements showing strong emission intensities it is comparable to ICP-MS systems, since 20 ng/g calcium contained in 100 droplets of 280 pl volume correspond to an absolute amount of only 560 fg calcium.

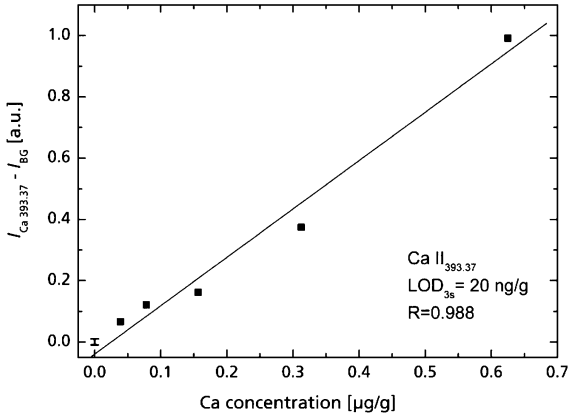

Fig. 8. Calibration curve for calcium. Experimental parameters: delay time t_{delay} = 1.5 μs, integration gate width $t_{int.}$ = 50 μs, laser pulse energy 140 mJ, pulse width 10 ns, 100 droplets contribute to one measurement, 20 measurements were accumulated for each concentration. Limit of detection (LOD) = 20 ng/g, correlation coefficient R = 0.988.

The analytical sensitivity is strongly dependent on the excitation and emission characteristics of the corresponding element. The excitation energy and the Einstein coefficient determine together with the plasma properties the emission intensity of the respective line of any element. Calcium belongs to the group of elements showing strong line emission yielding a low limit of detection. Similar elements are aluminum, boron, cadmium, chromium, copper, magnesium, sodium and zinc. Here limits of detection below 1 ppm can be expected. Weak emission intensities were detected for the elements arsenic, cobalt, mercury, lead, platinum, selenium and tin. Here the corresponding limits of detection are higher, with our set up we expect values between 20 and 100 ppm. Between these two groups the elements iron, nickel, silicon, titanium and vanadium can be found with limits of detection in the low ppm region. The elements were classified by comparing signal-to-noise values from echelle spectra recorded under identical conditions.

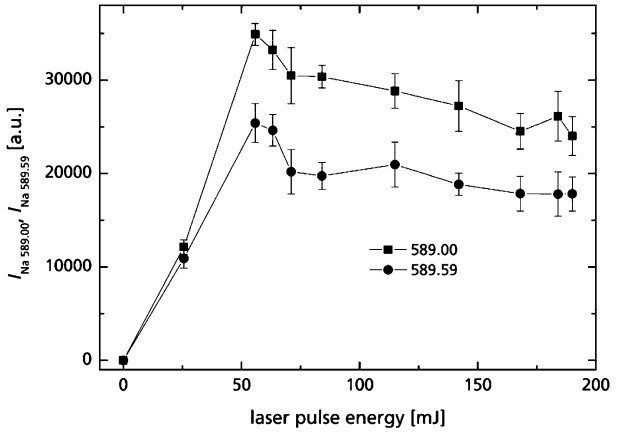

Fig. 7. Line intensities $I_{Na\ 589.00}$ and $I_{Na\ 589.59}$ versus laser pulse energy. Sample: droplets containing 500 ppm sodium. 50 laser pulses were accumulated. A maximum is observed at approximately 60 mJ per pulse.

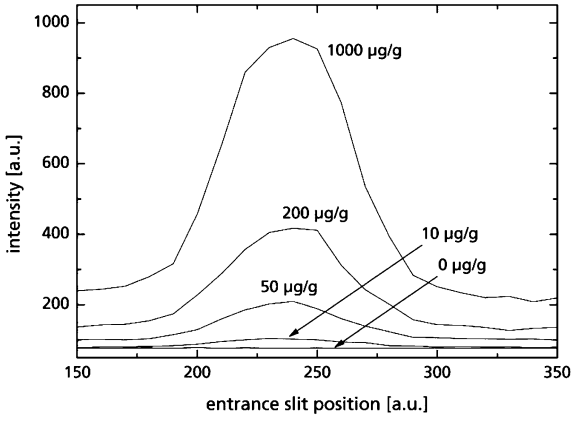

Fig. 9. Shape of the Cu I 324.75 nm line, recorded with the Paschen–Runge spectrometer by tilting the refractory plate behind the entrance slit. The concentrations of the different samples are given at the curves.

3.4. Shape of copper transitions, measured with the Paschen–Runge spectrometer

In the normal mode of operation the Paschen–Runge spectrometer can only detect the intensity of radiation in very narrow spectral windows defined by the resolution of the instrument and the positions of the photomultipliers, respectively the exit slits. Scanning over a narrow spectral region (less than one nanometer) is possible by tilting a refractory plate positioned directly behind the entrance slit. The tilting moves the incoming beam and tunes all spectrometer channels to a shifted wavelength. The Paschen–Runge spectrometer is equipped with a stepper motor that allows the precise tilting of this plate. Plotting the photomultiplier intensity against the stepper motor position gives the spectral shape of the respective transition. Fig. 9 shows the line shape for different concentrations of copper samples between 10 and 1000 ppm.

3.5. Continuous flow measurement of a magnesium sample

In order to simulate a chromatographic separation we made continuous flow measurements by connecting the droplet generator to an HPLC-pump that forces a constant liquid flow (typically 5–15 μl/min) through the glass capillary. For the stability of the droplet production it is important to adapt the volume flow of the droplet generator to the volume flow delivered by the pump. Otherwise the droplet generator may either run dry or droplet formation may fail because too much liquid is delivered to the glass capillary. In order to match the volume flows of the HPLC-pump and the droplet generator, an active closed loop controlled the droplet frequency. A liquid flow of 13 μl/min is equivalent to a droplet frequency of 800 Hz (droplet volume 270 pl). Because the laser was operated at 10 Hz a pulse divider was used to reduce the measurement frequency to 10 Hz. A six-way switching valve (Rheodyne) integrated into the flow system in front of the droplet generator allowed us to inject small amounts of sample (20 μl) without interrupting the droplet stream. Monitoring the signal intensity of the sample element as a function of time delivered a signal peak comparable to signals detected in chromatographic separations. Because of dead volumes in the droplet generator and in the adapter tubes used for connecting the capillary and the droplet generator a temporal peak broadening is detected. Fig. 10 shows a continuous flow measurement of 20 μl of a sample containing 18 ppm magnesium. The total amount of analyzed magnesium that gives rise to the signal shown is 4.2 ng because only one out of 85 droplets was analyzed due to the mismatch in droplet and laser frequency.

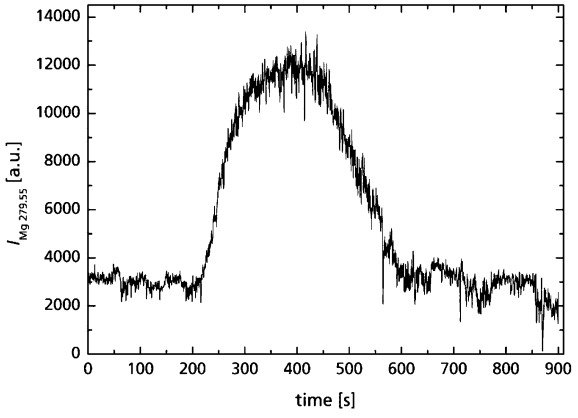

Fig. 10. Continuous flow measurement of 20 μl of 18 μg/g Mg solution. The sample was injected in the continuous solvent flow coming from the HPLC-pump with the aid of a Rheodyne 6-way valve. Temporal broadening of the peak can be seen as a result of dead volumes in the system. The droplet frequency was 850 Hz, the measurement frequency was 10 Hz. The analyzed amount of sample is 4.2 ng. The data are smoothed with a 10 point moving average function.

4. Conclusions

A piezoelectric droplet generator and a LIBS analysis of single droplets for applications in the speciation analysis were combined and tested successfully. Single, isolated droplets with sub-nanoliter volumes are detected by a photodiode and were evaporated and transformed into a hot plasma by irradiation with synchronized laser pulses. The Paschen–Runge spectrometer employed allows fast measurement frequencies with simultaneous single pulse evaluation for up to 33 photomultiplier channels. For sensitive elements (Ca, Na) limits of detection in the ppb range were achieved. The coupling of the droplet generator to an HPLC pump that forces a defined flow through the nozzle was realized with the aid of an active closed loop to control the droplet frequency and adapt it to the volume flow given by the pump.

The temporal and spatial overlapping of droplet and laser pulse is one of the most important aspects of the experiment because slight misalignments give rise to large declines in signal. The long term stability of the adjustment is a critical factor. Temporal stability can be achieved by triggering the laser relative to the precise detection of a droplet with the photodiode, spatial stability can be achieved by very clean droplet generators and particle-free liquid samples. Filtering of the samples through filters with not more than 0.2 μm pore size is strongly recommended.

The results show the potential of the piezoelectric droplet principle for the development of new detectors for ultra low volume flow separation techniques such as micro-HPLC or capillary electrophoresis. Volume flows in the sub μl/min region will be accessible without dilution of the sample.

Acknowledgements

The authors thank the German Bundesministerium für Bildung, Forschung und Technologie (BMBF), the Fraun-

hofer Society, and national industrial partners for financial support.

References

[1] R. Knopp, F.J. Scherbaum, J.I. Kim, Laser induced breakdown spectroscopy (LIBS) as an analytical tool for the detection of metal ions in aqueous solutions, Fresenius' J. Anal. Chem. 355 (1996) 16–20.
[2] B. Welz, Speciation analysis: where is it going? An attempt at a forecast, Spectrochim. Acta, Part B: Atom. Spectrosc. 53 (1998) 169–175.
[3] R. Lobinski, J. Szpunar, Biochemical speciation analysis by hyphenated techniques, Anal. Chim. Acta 400 (1999) 321–332.
[4] A.R. Timerbraev, Element speciation analysis by capillary electrophoresis, Talanta 52 (2000) 573–606.
[5] see for example WWW.agilent.com.
[6] D. Beauchemin, Inductively coupled plasma mass spectrometry, Anal. Chem. 74 (2002) 2873–2894.
[7] P.K. Kenedy, D.X. Hammer, B.A. Rockwell, Laser induced breakdown in aqueous media, Prog. Quantum Electron. 21 (1997) 155–248.
[8] R. Knopp, F.J. Scherbaum, J.I. Kim, Laser induced breakdown spectroscopy (LIBS) as an analytical tool for the detection of metal ions in aqueous solutions, Fresenius' J. Anal. Chem. 355 (1996) 16–20.
[9] P. Fichet, P. Mauchien, J.F. Wagner, C. Moulin, Quantitative elemental determination in water and oil by laser induced breakdown spectrometry, Anal. Chim. Acta 429 (2001) 269–278.
[10] W.F. Ho, C.W. Ng, N.H. Cheung, Spectrochemical analysis of liquids using laser induced plasma emission: effects of laser wavelength, Appl. Spectrosc. 51 (1997) 87–91.
[11] J.E. Carranza, B.T. Fisher, G.D. Yoder, D.W. Hahn, On-line analysis of ambient air aerosols using laser-induced breakdown spectroscopy, Spectrochim. Acta, Part B: Atom. Spectrosc. 56 (2001) 851–864.
[12] H.A. Archontaki, S.R. Crouch, Evaluation of an isolated droplet sample introduction system for laser-induced breakdown spectroscopy, Appl. Spectrosc. 42 (1988) 741–746.
[13] G. Arca, A. Ciucci, V. Palleschi, S. Rastelli, E. Tognoni, Trace element analysis in water by laser-induced breakdown spectroscopy technique, Appl. Spectrosc. 51 (1997) 1102–1105.
[14] A.E. Pichahchy, D.A. Cremers, M.J. Ferris, Elemental analysis of metals under water using laser-induced breakdown spectroscopy, Spectrochim. Acta, Part B: Atom. Spectrosc. 52 (1997) 25–39.
[15] R.L. Vander Wal, T.M. Ticich, J.R. West, P.A. Householder, Trace metal detection by laser-induced breakdown spectroscopy, Appl. Spectrosc. 53 (1999) 1226–1236.
[16] A. Kuwako, Y. Uchida, K. Maeda, Supersensitive detection of sodium in water with use of dual-pulse laser-induced breakdown spectroscopy, Appl. Opt. 42 (2003) 6052–6056.
[17] K.M. Lo, N.H. Cheung, ArF Laser-induced plasma spectroscopy for part-per-billion analysis of metal ions in aqueous solution, Appl. Spectrosc. 56 (2002) 682–688;
X.Y. Pu, W.Y. Ma, N.H. Cheung, Sensitive elemental analysis of aqueous colloids by laser-induced plasma spectroscopy, Appl. Phys. Lett. 83 (2003) 3416–3418.
[18] H. Ulmke, T. Wriedt, H. Lohner, K. Bauckhage, The piezoelectric droplet generator—a versatile tool for dispensing applications and calibration of particle sizing instruments, Precis. Eng. - Nanotechnology, Proceedings of the 1st International Euspen Conference, vol. 2, Shaker Verlag, Aachen, 1999, pp. 290–293.
[19] R. Noll, H. Bette, A. Brysch, M. Kraushaar, I. Mönch, L. Peter, V. Sturm, Laser-induced breakdown spectrometry—applications for production control and quality assurance in steel industry, Spectrochim. Acta, Part B: Atom. Spectrosc. 56 (2001) 637–649.
[20] L.I. Sedov, Similarity and dimensional methods in mechanics, in: M. Holdt (Ed.), Gostekhizdat, Moscow, 1957, 4th ed., Academic Press, New York, 1959, English transl.
[21] R. Noll, R. Sattmann, V. Sturm, S. Winkelmann, Space and time-resolved dynamics of plasmas generated by laser double pulses interacting with metallic samples, J. Anal. At. Spectrom. 19 (2004) 419–428.
[22] In accordance with DIN 32645 (German Industrial Standard: decision limit, detection limit and determination limit. Estimation in case of repeatability, terms, methods, evaluation. Beuth Verlag, Berlin, Germany 1994).